## **TOPICAL COLLECTION: ELECTRONIC PACKAGING AND INTERCONNECTIONS 2022**



# Sn Whisker Growth During Mechanical Loading and Unloading: Highlighting the Critical Role of Stress in Whisker Growth

Piyush Jagtap<sup>1,2</sup> ● · Nupur Jain<sup>1</sup> · Allan Bower<sup>1</sup> · Eric Chason<sup>1</sup>

Received: 1 June 2022 / Accepted: 8 November 2022 / Published online: 8 December 2022 © The Minerals, Metals & Materials Society 2022

#### Abstract

Whisker formation in metallic coatings has been studied extensively over the past few decades. A wide consensus exists for stress as a driving force behind whisker growth. However, many of the details are not understood, and other theories have been proposed that challenge stress-based explanations. In this paper, we quantify the kinetics of stress-driven whisker growth by demonstrating that the whisker growth can be turned on and off by application and removal of mechanical load. We observed that (i) whiskers formed during the loading stage grow linearly with time, (ii) they stop growing soon after the load was removed, and (iii) they resume growth when the load was reapplied. The experimental results are explained using finite element analysis (FEA) of stress evolution due to applied load and average growth rate predictions. The results have implications for applications in which the coatings experience stresses, for example, due to fasteners or thermal cycling.

**Keywords** Sn coatings · whisker growth · mechanical loading · stress · FEA

## Introduction

Whisker growth in metallic coatings continues to pose a risk in electronic components.<sup>1,2</sup> Sn-based systems, in particular, have been vastly studied over several decades to understand the mechanisms behind whisker growth, and yet a concrete understanding of this complex phenomenon and hence engineering solutions to prevent its growth remains elusive.<sup>3-5</sup> The problem due to whisker growth has re-emerged after a ban on Pb in the processing of electronic components back in 2006.6 More recently, studies have shown whisker growth from Pb-free micro-solder arrays, 7 other metals and alloys such as MAX phases.8 Therefore, there is renewed interest in understanding the driving forces behind whisker growth. A plethora of experimental 9-17 and numerical 18-21 evidence now exists suggesting that compressive stress in Sn films drives the nucleation and growth of Sn whiskers. However, recent theories<sup>8,22-24</sup> based on other driving forces such as electrostatic force or oxidation challenge stress-based

Compressive stress in Sn can originate from multiple sources including residual stress induced during the film deposition,<sup>25</sup> formation of the intermetallic compound (IMC) Cu<sub>6</sub>Sn<sub>5</sub> in Sn-Cu systems, <sup>9,21,26–31</sup> thermal expansion mismatch between Sn film and substrate, 14,32-35 oxidation reactions in Sn alloys, 23,36-42 and mechanical loading of the Sn film surface. 43-52 In the case of Cu/Sn systems, which are of general interest, IMC growth and mechanical loading can provide a sustained driving force enabling whisker growth over a long period. Other sources of stress, such as residual stress from deposition, thermal expansion, and stress due to oxidation are not sustained over prolonged periods and the stress decays rapidly due to relaxation via creep deformation, thereby reducing the driving force available for whisker growth. Moreover, due to multiple processes contributing to stress generation as well as relaxation, the stress in Sn changes rapidly with time and hence requires real-time monitoring.

Several studies have been performed to quantify the whisker growth kinetics in relation to the stress state in Sn and Sn-based systems. <sup>13,33,53–56</sup> However, in most of the



interpretation, and hence a fundamental driving force for Sn whisker growth is still under debate. This is mostly because quantitative studies directly relating whisker nucleation and growth to stress as a driving force have remained challenging to perform.

Piyush Jagtap piyush.jagtap@msme.iith.ac.in

School of Engineering, Brown University, Providence, RI 02912, USA

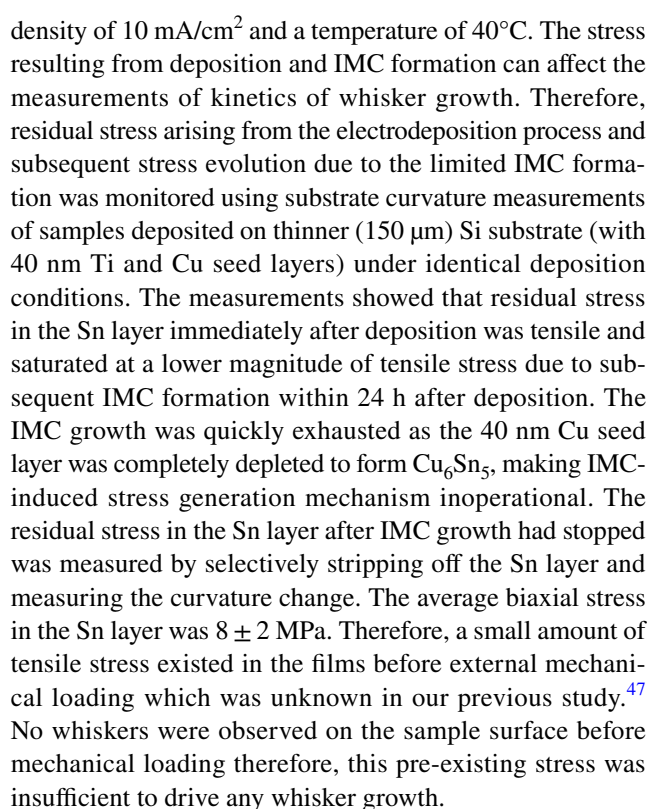
Materials Science and Metallurgical Engineering, Indian Institute of Technology, Hyderabad, Telangana 550082, India

previous studies, either the introduced stress could not be externally controlled, as in the case of IMC formation, <sup>57</sup> or the stress in the film could not be maintained for prolonged periods, such as in thermal studies where Sn films were heated to induce compressive stress, <sup>58,59</sup> limiting the scope of some of these experiments to just a few hours during which whisker kinetics could be monitored. <sup>53</sup> Other studies have been carried out to grow whiskers under the application of a mechanical load. However, either the applied load was not isolated from the IMC-induced stress <sup>51</sup> or the studies relied on the removal of the applied load for direct observation of whiskers, <sup>49,50</sup> making it difficult to directly relate the driving force and whisker growth kinetics.

We recently developed an experimental methodology that allowed us to circumvent some of these issues and monitor whisker nucleation and growth in real time. 47 A miniaturized clamping fixture was designed to apply a controlled mechanical load on a small area on the Sn surface using a flat punch indenter. The applied load can be maintained for extended periods and can be monitored using a force sensor integrated with the fixture. The applied mechanical load can also be removed and reapplied at any time. Furthermore, due to its small size, the fixture can be mounted inside a scanning electron microscope (SEM) chamber to periodically monitor the film surface for whisker growth. More details of the fixture and procedure adopted for measuring the kinetics of whisker growth in Sn thin films can be found in our previous work. 47 In that work, 47 we studied the growth kinetics of the whiskers under a constant load. It was observed that many whiskers stopped prematurely after an initial period of linear growth, while a few of them continued to grow as long as the applied load was maintained. To ensure that the applied load drives the whisker growth and that premature stopping of whisker growth was related to other microstructural aspects such as grain structure and orientation at the whisker root, we perform experiments with a loading and unloading cycle. In the present work, we examine the role of stress in Sn whisker growth during a mechanical loading-unloading cycle. The results highlight a crucial link between stress and whisker growth and may resolve the much-debated role of compressive stress in whisker growth.

## **Experimental Procedure**

Sn-coated samples were prepared on 1 mm thick glass substrates. The glass surface was first cleaned and was subsequently coated with a 40 nm Ti adhesion layer followed by a 40 nm Cu layer by evaporation. This thickness of Cu was selected to significantly limit the formation of IMC at the Sn/Cu interface. Sn film of 2.5  $\mu$ m thickness was then electrodeposited using a stannous sulfate electrolytic solution. The deposition was conducted at a constant current



The actual samples (Sn/Glass substrate) were aged in ambient conditions for 48 h before mechanical loading so that IMC-induced stress did not interfere with the measurements of whisker growth under mechanical loading. A stainless-steel buffer piece was glued on the sample surface using superglue to ensure uniform loading on an otherwise rough surface of electrodeposited Sn. The sample was mounted on the loading fixture, and a small area of the film surface ~ 3 mm<sup>2</sup>, as shown in Fig. 1, was subjected to a loading, unloading and reloading sequence. During the first loading stage, the film was subjected to a fixed load which was held constant for 48 h. The load was then removed completely, and the sample was kept unloaded for the next 24 h. Following this interruption in loading, the sample was reloaded back to the same load as in the initial loading stage. The applied load was measured using a force sensor (load range: 0-444.82 N) integrated with the loading assembly. The sensor was calibrated using standard weights and measuring the resistance change before the experiments. The mechanically applied load on the Sn surface  $(A = 3 \text{ mm}^2)$  was equivalent to 28 MPa of pressure as shown schematically in Fig. 1, i.e., at x = 0,  $\sigma(x) = \Sigma = -28$  MPa. Here,  $\Sigma$  is the uniform pressure under the punch and the negative sign indicates the applied pressure was compressive. Due to creep relaxation and grain boundary diffusion, a uniform hydrostatic stress state  $\sigma(xx) = \sigma(yy) = \sigma(zz) = -\Sigma$  exists in the film under the pressurized region.

The film surface, up to  $80\,\mu m$  from the region where the load was applied, was monitored for whisker nucleation and



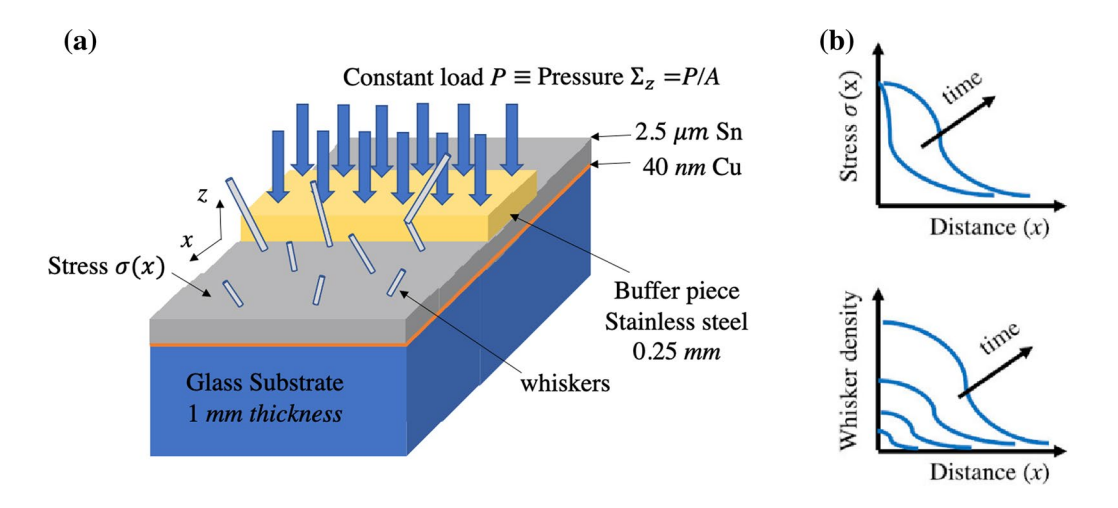


**Fig. 1** (a) Schematic illustration of loading assembly used in the experiments. A constant load (P) equivalent to a pressure of  $\Sigma = P/A$  is maintained on the Sn surface, where A is the pressurized area. A uniform hydrostatic stress state exists in the film under the pressurized region. Because of the diffusion of Sn atoms via grain bounda-

ries from the compressive region under the punch to the surrounding region, the stress  $\sigma(x)$  spreads out in the surrounding region, i.e., adjacent to a pressurized area. The stress  $\sigma(x)$  and whisker density in the adjacent area evolves with time as shown in (b). Note that at x=0,  $\sigma(x)=\Sigma$ , =-28 MPa.

growth using an SEM at regular time intervals throughout the sequence of load application. The sample was stored in ambient conditions between the imaging sessions. Multiple whiskers were monitored over the Sn surface in real time during the SEM observations. To determine the actual lengths of whiskers from 2D projections such as SEM images, we adopt the following procedure. First, the whisker is imaged at a fixed tilt angle  $\theta$ . The whisker is imaged again after a 90° rotation about the sample normal. This changes the coordinates of whisker from  $(x'_1, y'_1)$  to  $(x'_2, y'_2)$  in a projection plane with basis vectors (x', y'). The coordinates of a whisker in its projection plane can be easily extracted from the SEM images. The coordinates of the whisker in the projection plane can be related to its true coordinates in the sample reference frame using a coordinate transformation with a appropriate transformation matrix. This allows a correction to be made for the length of the whiskers estimated from the 2D images. A similar approach was used in previous studies.<sup>9,61</sup> An additional advantage of the real-time observation of whisker growth is that it allows us to determine the incremental increase in the length of a whisker and observe whiskers as they kink. This allows us to determine the true lengths of whiskers even if they are kinked. The whisker volume was estimated assuming a cylindrical shape.

## **Results and Discussion**

The real-time whisker nucleation and growth observations made during the loading phase were consistent with the results reported in our previous work.<sup>47</sup> Nucleation density was higher closer to the edge of the pressurized region,

where the compressive stress was higher. Over time, nucleation spread to larger distances from the edge as the compressive stress built up in the surrounding region as illustrated in Fig. 1b. The results of nucleation kinetics are not reported here; details can be found in previous works. 47,62 During aging under the applied load, a significant fraction of the total nucleated features grew into regular filament-type whiskers (with constant diameter) along with a few hillocks (which had continuous growth at the base). The whisker and hillocks continued to grow until 48 h, at which time the applied load was removed. The unloading resulted in a loss of driving force, and hence all whiskers and hillocks stopped their growth after unloading and remained inactive for the period of interruption until the film was reloaded. Several whiskers were imaged just before unloading and immediately after unloading. The length of whiskers remained unchanged, indicating that they stop their growth on a very short time scale. Figure 2 shows representative time-lapse SEM images of one such whisker and hillock during a loading sequence, showing a pause in the growth over 24 h (from t=48 h to t=72 h) when the load was removed, followed by a resumption in growth when the load was reapplied. The measurement of whisker volume, as shown in Fig. 2b, indicates that the volume of an individual whisker increased linearly with time, i.e., with a constant growth rate. The growth rate dropped to zero upon unloading. Upon reloading, the whisker growth resumed but the growth rates were different by a factor of 2–3 depending on the distance of the whiskers from the edge. The experiments demonstrate that the whisker growth can be stopped and resumed by controlling the applied load and therefore is fundamentally linked with



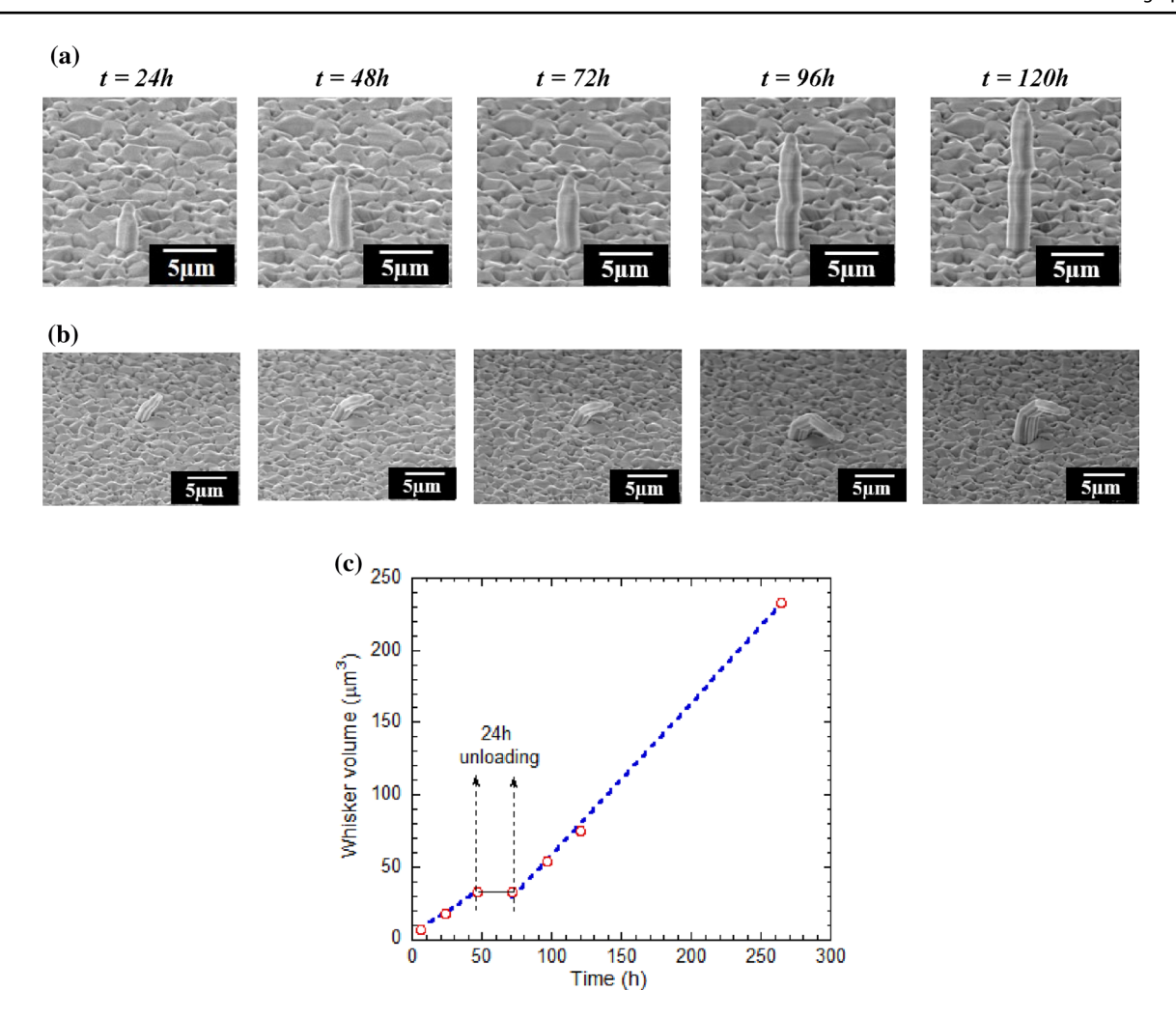


**Fig. 2** (a) A whisker and (b) hillock growth sequence captured at a different time (t) after mechanical loading. The sample remained unloaded between t=48 h to t=72 h, following which it was reloaded

to the same applied load. (c) The volume of a whisker shown in (a) is estimated from SEM images with time.

the compressive stress in the film created by the applied load.

It should be noted that only whiskers with a constant cross-sectional area (i.e., whiskers with constant diameter) were used to calculate the average volume. The growth of hillocks with continuous expansion at the base (see Fig. 2b) was also observed. It was difficult to determine the volume of such irregularly shaped features. The growth kinetics of a total of 26 whiskers spread over an 80  $\mu m$  distance from the edge was monitored using SEM imaging. The majority of these whiskers grew in the region within the first 30  $\mu m$  from the pressurized edge.

The film surface under observation was segmented into multiple 10 µm bands at increasing distances from the pressurized edge in the same way as described in our previous work.<sup>47</sup> The volume measurements of individual whiskers lying within these bands were used to calculate the average growth rate of whiskers at different distances from the

edge. The average volume of whiskers with time is plotted in Fig. 3a. The average growth rates of the whiskers varied with their position from the pressurized edge. In general, whiskers closer to the edge grew at a faster rate than the whiskers further away. This is consistent with the previously reported findings in <sup>47</sup> and supported by the analysis of stress which decays with distance from the edge. <sup>62</sup>

The linear growth rates of whiskers before unloading and after reloading suggest that the underlying mechanism of growth remains unaffected by the load interruption. Since the focus of the present study was to look at growth kinetics of whiskers before, during, and after the load interruption, only the whiskers that began to grow in the first loading phase were used for calculating the average volume shown in Fig. 3a. It is important to point out that new whiskers also formed once the sample was reloaded after a 24 h interruption. A total of 12 new whiskers (spread over 80 µm distance



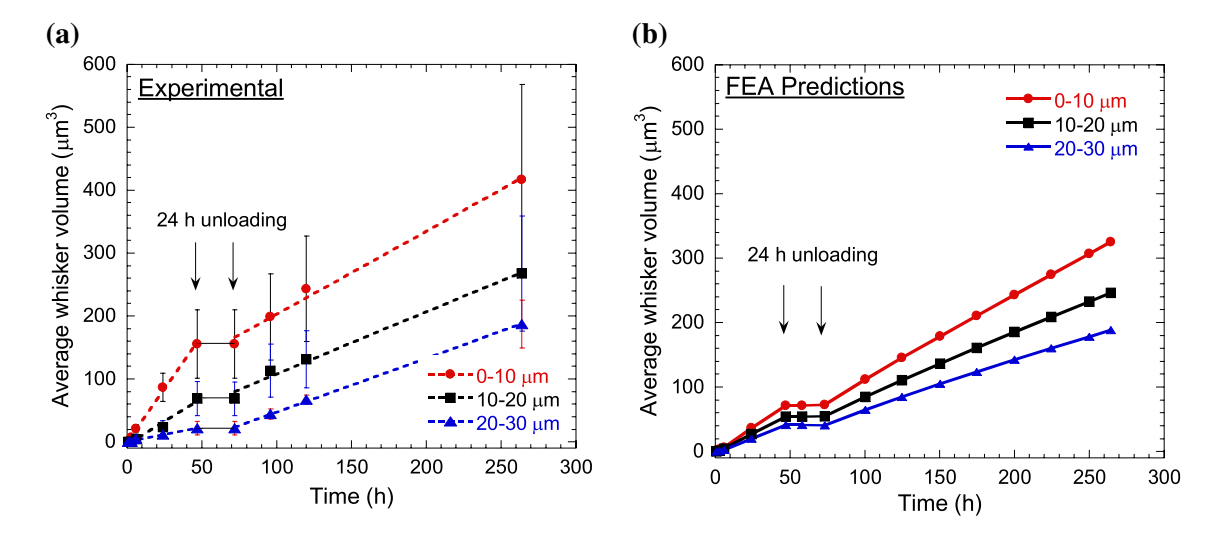


Fig. 3 (a) Experimentally measured average whisker growth rates at different distances from the region where the load was applied; (b) FEA predictions of the average whisker growth rates. The vertical arrows in (a) indicate the period for which the applied load was removed for 24 h.

from the pressurized edge) were observed after the reloading at t = 72 h.

While the applied stress on the area under the punch ( $\sigma_{xx} = \sigma_{yy} = \sigma_{zz} = -\Sigma$ ) remained constant, the stress field in the surrounding region ( $\sigma_{xx} = \sigma_{yy} = -\sigma(x,t)$ ) continuously evolve with time, as shown schematically in Fig. 1b. To relate the experimentally measured rate of growth to its driving force (i.e., compressive stress field  $-\sigma(x,t)$  in the surrounding), a finite element analysis (FEA) was performed. The details of the FEA model have been described previously,  $^{62}$  so it is only briefly summarized here. The FEA model considers an isotropic Sn layer attached to a much thicker rigid glass substrate. Therefore, applied strain is accommodated by elastic, plastic, and diffusive processes in the Sn layer. The total in-plane strain must always be zero, since the lateral displacements are not allowed by a rigid substrate. This gives a condition

$$\dot{\varepsilon_e} + \dot{\varepsilon_p} + \dot{\varepsilon_d} = 0 \tag{1}$$

By substituting individual contributions to the strain rates from elastic, plastic, and diffusive processes, we get Eq. 2. Here,  $\dot{\varepsilon_e}$  is the in-plane elastic strain rate related to stress rate using a biaxial modulus. Since the experiments were performed at constant ambient temperature, and whisker growth does lead to shrinkage in the out-of-plane direction, the biaxial modulus of Sn remains constant. The average stress can be obtained by solving the following differential equation  $^{62}$ 

$$\frac{1}{M}\frac{d\sigma}{dt} - \frac{1}{3}\left(\frac{\Omega\overline{D}}{kT}\right)\frac{\partial^2\sigma}{\partial x^2} + \dot{\varepsilon}_p(\sigma) = 0$$
 (2)

The plastic strain rate  $\dot{\epsilon_p}$  was defined using the power-law creep equation given by

$$\dot{\varepsilon_p} = \varepsilon_o \exp\left(-\frac{Q_{cr}}{kT}\right) \left(\frac{|\sigma|}{\sigma_o}\right)^m \left(\frac{3S_{ij}}{2\sigma_e}\right) \tag{3}$$

where,  $S_{ii}$  is the deviatoric component of the stress tensor,  $\sigma_{e}$ is the von Mises stress,  $\sigma_o$  is the nominal yield stress,  $Q_{cr}$  is the activation energy of the creep, and m is the stress exponent. The creep parameters were determined by modeling the above equation on the experimentally measured stress relaxation of the thermally strained Sn coatings used in the study having identical grain size and thickness, and similar loading rate. The details of modeling stress relaxation in Sn can be found in Shin and Chason.<sup>63</sup> The values of activation energy of creep and creep stress exponent obtained from curve fitting were in good agreement with the ones reported previously in the literature. The diffusion in beta-Sn is quite complicated, and it depends on the microstructure, amount of impurities, texture, stress, etc. Since we do not have experimental Sn diffusivity data for Sn coatings used in our work, we used values of  $D_o$  and  $Q_{gb}$  reported in the literature. The model considers the average stress at length scales much larger than the spacing between the whiskers, and it also considers a critical/threshold stress for whisker growth  $(\sigma_{crit})$  at the whisker root to predict the growth rates. If the average stress  $\sigma(x, t) > \sigma_{crit}$ , diffusion of Sn atoms towards the whisker root can occur, and growth rates can be predicted.<sup>62</sup>

To model the experimental results, the model was modified to turn on and turn off the applied load and analyze the evolution of the stress field in the region, adjacent to where the load was applied. The kinetic parameters used in



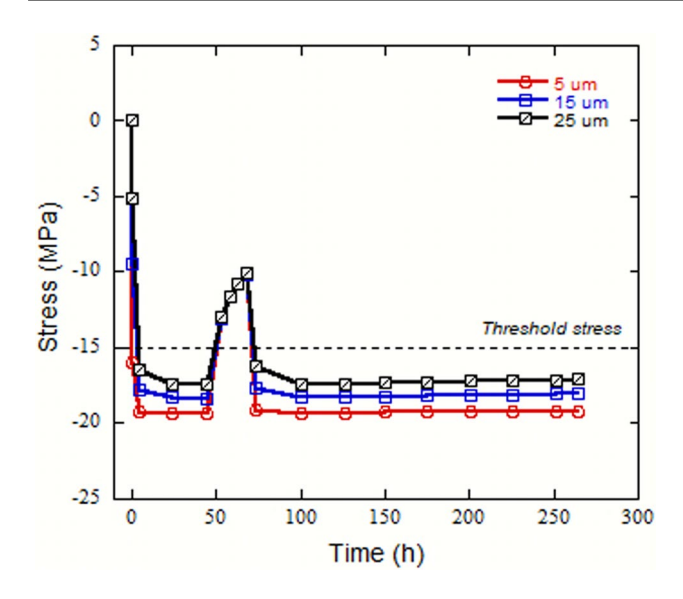


**Fig. 4** The FEA predictions of stress evolution at different distances from the pressurized edge during loading (t=0 h), unloading (t=48 h), and reloading (t=72 h) sequence.

the model including the activation energy for creep, power-law creep exponent, grain boundary diffusivity, and critical stress for whisker growth can be found in Jain et al. <sup>62</sup>

Figure 4 shows the evolution of compressive stress with time at several distances from the edge of the pressurized region. The distance, shown in the legend, corresponds to the center of the bands where whisker growth was monitored in the measurements. At t=48 h, when the applied load is removed, the compressive stress decreases rapidly (i.e., becomes more tensile) and quickly falls below the threshold stress magnitude required to sustain whisker growth ( $\sim -15$  MPa, which was determined through thermally induced stress measurements<sup>53</sup>). This explains the prompt stop in the growth of whiskers observed in Fig. 2. At t=72 h, when the load is reapplied, the compressive stress increases rapidly and quickly reaches a steady state. This sustained elevated state of stress provides a continuous driving force that enables the whiskers to grow further.

It is important to note that the stress recovery after reloading was faster than the stress relaxation after unloading. The FEA model allows us to evaluate the contribution to the stress from individual processes considered in the model. It was observed that stress ( $\sigma(x,t)$ ) after loading was dominated by diffusion of Sn atoms via grain boundaries. Interestingly, the stress after unloading decayed faster near the pressurized edge compared to far away from it. This can be attributed to power-law creep, where a higher stress level near a pressurized edge leads to faster stress relaxation. The time scales for stress relaxation upon unloading and recovery after reloading are very short, consistent with the experimental observations.



**Table I** The comparison of whisker growth rates captured through experiments and modeling shown graphically in Fig. 3

Distance (x)	Average growth rate		
	0–10 μm	10–20 μm	20–30 μm
Experiment (before interrupt)	$3.2  \mu \text{m}^3/h$	1. 48 μm <sup>3</sup> /h	$0.46  \mu \text{m}^3/h$
Experiment (after interrupt)	$1.14  \mu m^3/h$	$0.98  \mu \text{m}^3/h$	$0.85  \mu \text{m}^3/h$
FEA (before and after interrupt)	$1.3  \mu \text{m}^3/h$	$0.99  \mu\mathrm{m}^3/h$	$0.76\mu\mathrm{m}^3/h$

The whisker volume estimations were used to understand the kinetics of growth instead of whisker length because the rate at which length increases depends on the diameter of a whisker. Additionally, the rate of change of volume can be directly related to the driving force (i.e., stress) using the following relation

$$\frac{\partial V}{\partial t} = -\nabla . D\nabla \sigma \tag{4}$$

The average volume estimations from FEA (see Fig. 3b) agree reasonably well with the experimentally measured whisker volumes. The average growth rates at different distances from the pressurized edge obtained by a linear fit to the data are tabulated in Table I.

The experimentally measured growth rates, before unloading, were higher than the FEA predictions near the pressurized edge. Interestingly, after reloading, the growth rates measured from experiments and predicted by FEA were more consistent. The average growth rate after reloading decreased because a few whiskers suddenly stopped after a period of linear growth while the rest of them grew continuously until the load was maintained. The disagreement between FEA and experiments at least initially may be because the FEA considers a fixed number density of whiskers to estimate average volume. The situation in experiments is more complex. For example, several new whiskers were formed after reloading, while a few old whiskers suddenly stopped growing. The average volume measurements shown in Fig. 3a do not include newly formed whiskers and irregular features like hillocks. Nevertheless, trends in FEA predictions and experimental measurements are promising.

The study highlights that the mass transport of Sn atoms towards the whisker root is essential to sustain its growth. The applied pressure on the Sn surface sets up a compressive stress field in the vicinity of the area where the load was applied. The average compressive stress increases with time as Sn atoms diffuse away from the area under the load. Once a threshold stress value is reached whisker growth can occur. Alternative whisker growth theories based on other driving forces such as electrostatic force, <sup>22,64,65</sup> surface oxidation and corrosion, <sup>23,66,67</sup> and compositional gradients <sup>8,24,68</sup> were also proposed in other works. But experimental measurements of

the kinetics of whisker growth by controlling the proposed driving forces are not available. Although the stress-driven diffusion mechanism for whisker growth is widely accepted, conclusive evidence such as manipulating whisker growth by controlling the applied stress is extremely rare<sup>45</sup> due to the difficulty in performing such experiments. The interrupted load experiments and its FEA modeling clearly show that the compressive stress in Sn is the necessary driving force for whisker growth. Additionally, it also highlights the extremely short time scales over which stress can relax and recover in Sn owing to its low melting point and fast atomic diffusion.

# **Conclusion**

To understand the response of whisker growth to stress, we have controlled and/or characterized the compressive stress in the Sn layer due to multiple sources: (i) applied load, (ii) Cu-Sn IMC growth (by limiting IMC formation using very thin Cu underlayer), (iii) residual stress coming from electrodeposition (by optimizing deposition parameters and quantifying the residual stress), and (iv) thermal stress due to thermal expansion mismatch between Sn film and the glass substrate (by avoiding large temperature changes during storage). This allowed a direct correlation between the compressive stress and the measured whisker growth rates. The applied load can be maintained for a long period to sustain long-term whisker growth or can be turned off to interrupt the whisker growth. The FEA was used to model the compressive stress around whiskers as well as for predictions of the average whisker growth rates. The FEA results highlight that the stress generation and relaxation due to the mechanical loading and unloading were mainly governed by grain-boundary diffusion of Sn atoms and power-law creep processes which are sufficiently rapid to cause the rise and drop in the stress on a sufficiently small time scale. Once the stress drops below a threshold stress value, whisker growth stops completely, and it resumes as the elevated state of stress is re-established. The rapid evolution of stress shown by the modeling also highlights how stress induced in coatings used in applications, for instance by fasteners, can be an important source of whisker formation.

**Acknowledgments** The authors gratefully acknowledge the support of the NSF DMR under Contract DMR-1903071.

Funding National Science Foundation, DMR-1903071

Conflict of interest On behalf of all authors, the corresponding author states that there is no conflict of interest.

#### References

- "NASA tin whisker webpage https://nepp.nasa.gov/whisker/," NASA tin whisker webpage https://nepp.nasa.gov/whisker/, Accessed June 2021
- H. Leidecker and J. Brusse, "Tin whiskers: a history of documented electrical system failures," Space Shuttle Program Office, 2006
- 3. G.T. Galyon, "Annotated tin whisker bibliography and anthology. *IEEE Trans. Electron. Packag. Manuf.* 28, 94–122 (2005).
- E. Chason, N. Jadhav, F. Pei, E. Buchovecky, and A. Bower, Growth of whiskers from Sn surfaces: driving forces and growth mechanisms. *Prog. Surf. Sci.* 88, 103–131 (2013).
- P. Jagtap and P. Kumar, Whisker growth in Sn coatings: a review of current status and future prospects. *J. Electron. Mater.* 50, 735–766 (2021).
- E. Parliament, Directive 2011/65/EU of the European Parliament and of the Council of 8 June 2011 on the restriction of the use of certain hazardous substances in electrical and electronic equipment (RoHS). Off. J. Eur. Union 54, 88–110 (2011).
- Y. Li, M. Sun, S. Ren, H. Ling, T. Hang, A. Ming Hu, and M. Li, The influence of non-uniform copper oxide layer on tin whisker growth and tin whisker growth behavior in SnAg microbumps with small diameter. *Mater. Lett.* 258, 126773 (2020).
- 8. P. Zhang, Y. Zhang, and Z. Sun, Spontaneous growth of metal whiskers on surfaces of solids: a review. *J. Mater. Sci. Technol.* 31, 675–698 (2015).
- 9. B.Z. Lee and D.N. Lee, Spontaneous growth mechanism of tin whiskers. *Acta Mater.* 46, 3701–3714 (1998).
- K.N. Tu, J.O. Suh, A.T.C. Wu, N. Tamura, and C.H. Tung, Mechanism and prevention of spontaneous tin whisker growth. *Mater. Trans.* 46, 2300–2308 (2005).
- W.J. Boettinger, C.E. Johnson, L.A. Bendersky, K.W. Moon, M.E. Williams, and G.R. Stafford, Whisker and Hillock formation on Sn, Sn-Cu and Sn-Pb electrodeposits. *Acta Mater*. 53, 5033–5050 (2005).
- N. Jadhav, E.J. Buchovecky, L. Reinbold, S. Kumar, A.F. Bower, and E. Chason, Understanding the correlation between intermetallic growth, stress evolution, and Sn whisker nucleation. *IEEE Trans. Electron. Packag. Manuf.* 33, 183–192 (2010).
- 13. E. Chason, J. Vasquez, F. Pei, N. Jain, and A. Hitt, Quantifying the effect of stress on Sn whisker nucleation kinetics. *J. Electron. Mater.* 47, 103–109 (2018).
- F. Pei, E. Buchovecky, A. Bower, and E. Chason, Stress evolution and whisker growth during thermal cycling of Sn films: a comparison of analytical modeling and experiments. *Acta Mater.* 129, 462–473 (2017).
- P. Sarobol, J.E. Blendell, and C.A. Handwerker, Whisker and hillock growth via coupled localized Coble creep, grain boundary sliding, and shear induced grain boundary migration. *Acta Mater*. 61, 1991–2003 (2013).
- 16. J. Smetana, Theory of tin whisker growth: 'The end game.' *IEEE Trans. Electron. Packag. Manuf.* 30, 11–22 (2007).
- M. Sobiech, U. Welzel, E.J. Mittemeijer, W. Hügel, and A. Seekamp, Driving force for Sn whisker growth in the system Cu–Sn. Appl. Phys. Lett. 93, 011906 (2008).
- P. Jagtap, A. Chakraborty, P. Eisenlohr, and P. Kumar, Identification of whisker grain in Sn coatings by analyzing crystallographic micro-texture using electron back-scatter diffraction. *Acta Mater*. 134, 346–359 (2017).
- 19. A. Chakraborty and P. Eisenlohr, A full-field crystal plasticity study on how texture and grain structure influences hydrostatic stress in thermally strained  $\beta$ -Sn films. *J. Appl. Phys.* 124, 025302 (2018).



 Eric Buchovecky, "Numerical Simulation of Stress Generation and Whisker Growth in Sn Films" PhD Thesis Brown University (2010)

- E. Buchovecky, N. Jadhav, A.F. Bower, and E. Chason, Finite element modeling of stress evolution in Sn films due to growth of the Cu 6Sn 5 intermetallic compound. *J. Electron. Mater.* 38, 2676–2684 (2009)
- V.G. Karpov, Electrostatic theory of metal whiskers. *Phys. Rev. Appl.* 1, 044001 (2014).
- J.W. Osenbach, J.M. DeLucca, B.D. Potteiger, A. Amin, R.L. Shook, and F.A. Baiocchi, Sn corrosion and its influence on whisker growth. *IEEE Trans. Electron. Packag. Manuf.* 30, 23–35 (2007).
- Y. Zhang, C. Lu, Y. Dong, M. Zhou, J. Liu, H. Zhang, B. Ye, and Z.M. Sun, Insights into the dual-roles of alloying elements in the growth of Sn whiskers. J. Mater. Sci. Technol. 117, 65–71 (2022).
- M.E. Williams, K.W. Moon, W.J. Boettinger, D. Josell, and A.D. Deal, Hillock and whisker growth on Sn and SnCu electrodeposits on a substrate not forming interfacial intermetallic compounds. *J. Electron. Mater.* 36, 214–219 (2007).
- K.N. Tu, Interdiffusion and reaction in bimetallic Cu-Sn thin films. Acta Metall. 21, 347–354 (1973).
- K.N. Tu and J.C.M. Li, Spontaneous whisker growth on lead-free solder finishes. *Mater. Sci. Eng. A* 409, 131–139 (2005).
- N. Jadhav, E.J. Buchovecky, L. Reinbold, S. Kumar, A.F. Bower, and E. Chason, Understanding the correlation between intermetallic growth, stress evolution, and Sn whisker nucleation. *IEEE Trans. Electron. Packag. Manuf.* 33, 183–92 (2010).
- P. Jagtap, P. Ramesh Narayan, and P. Kumar, Effect of substrate composition on whisker growth in Sn coatings. *J. Electron. Mater.* 47, 4177–4189 (2018).
- A. Baated, K.S. Kim, and K. Suganuma, Effect of intermetallic growth rate on spontaneous whisker growth from a tin coating on copper. J. Mater. Sci. Mater. Electron. 22, 1685–1693 (2011).
- J. Hektor, J.B. Marijon, M. Ristinmaa, S.A. Hall, H. Hallberg, S. Iyengar, J.S. Micha, O. Robach, F. Grennerat et al., Evidence of 3D strain gradients associated with tin whisker growth. Scr. Mater. 144, 1–4 (2018).
- K. Suganuma, A. Baated, K.S. Kim, K. Hamasaki, N. Nemoto, T. Nakagawa, and T. Yamada, Sn whisker growth during thermal cycling. *Acta Mater.* 59, 7255–7267 (2011).
- F. Pei and E. Chason, In situ measurement of stress and whisker/ hillock density during thermal cycling of Sn layers. *J. Electron. Mater.* 43, 80–87 (2014).
- M. Dittes, P. Oberndorff, P. Crema, and V. Schroeder, Tin whisker formation in thermal cycling conditions. in *Proc. IPC-JEDEC Conf., Frankfurt, Ger.*, 105 (2003).
- Y. Wang, J.E. Blendell, and C.A. Handwerker, Evolution of tin whiskers and subsiding grains in thermal cycling. *J. Mater. Sci.* 49, 1099–1113 (2014).
- M. Dudek and N. Chawla, Oxidation behavior of rare-earth-containing Pb-free solders. J. Electron. Mater. 38, 210–220 (2009).
- M.A. Dudek and N. Chawla, Mechanisms for Sn whisker growth in rare earth-containing Pb-free solders. *Acta Mater*. 57, 4588– 4599 (2009).
- 38. M.A. Ashworth, D. Haspel, L. Wu, G.D. Wilcox, and R.J. Mortimer, An investigation into the effect of a post-electroplating electrochemical oxidation treatment on tin whisker formation. *J. Electron. Mater.* 44, 442–456 (2015).
- B. Illés and B. Horváth, Tin whisker growth from micro-alloyed SAC solders in corrosive climate. *J. Alloys Compd.* 616, 116–121 (2014).
- C.H. Su, H. Chen, H.Y. Lee, C.Y. Liu, C.S. Ku, and A.T. Wu, Kinetic analysis of spontaneous whisker growth on pre-treated surfaces with weak oxide. *J. Electron. Mater.* 43, 3290–3295 (2014).

- A.T. Wu and Y.C. Ding, The suppression of tin whisker growth by the coating of tin oxide nano particles and surface treatment. *Microelectron. Reliab.* 49, 318–322 (2009).
- S. Das Mahapatra and I. Dutta, Role of surface oxide in mitigating tin whisker growth: a finite element study. *Mater. Sci. Eng. A* 706, 181–191 (2017).
- 43. E. R. Crandall, G. T. Flowers, R. Jackson, P. Lall, and M. J. Bozack, "Growth of Sn whiskers under net compressive and tensile stress states. in *Electr. Contacts, Proc. Annu. Holm Conf. Electr. Contacts*, (2011)
- 44. F. Yang and Y. Li, Indentation-induced tin whiskers on electroplated tin coatings. *J. Appl. Phys.* 104, 113512 (2008).
- R. Fisher, L. Darken, and K. Carroll, Accelerated growth of tin whiskers. *Acta Metall.* 2, 368–373 (1954).
- 46. C.H. Pitt and R.G. Henning, Pressure-induced growth of metal whiskers. *J. Appl. Phys.* 35, 459–460 (1964).
- P. Jagtap, N. Jain, and E. Chason, Whisker growth under a controlled driving force: pressure induced whisker nucleation and growth. *Scr. Mater.* 182, 43–47 (2020).
- C.K. Lin and T.H. Lin, Effects of continuously applied stress on tin whisker growth. *Microelectron. Reliab.* 48, 1737–1740 (2008).
- S.K. Lin, Y. Yorikado, J. Jiang, K.S. Kim, K. Suganuma, S.W. Chen, M. Tsujimoto, and I. Yanada, Mechanical deformation-induced Sn whiskers growth on electroplated films in the advanced flexible electronic packaging. *J. Mater. Res.* 22, 1975–1986 (2007).
- H. Moriuchi, Y. Tadokoro, M. Sato, T. Furusawa, and N. Suzuki, Microstructure of external stress whiskers and mechanical indentation test method. *J. Electron. Mater.* 36, 220–225 (2007).
- J.J. Williams, N.C. Chapman, and N. Chawla, Mechanisms of Sn hillock growth in vacuum by in situ nanoindentation in a scanning electron microscope (SEM). J. Electron. Mater. 42, 224–229 (2013).
- I. Lujan-Regalado, A. Kirubanandham, J.J. Williams, and N. Chawla, Nucleation and growth of tin hillocks by in situ nanoin-dentation. *J. Electron. Mater.* 48, 58–71 (2019).
- F. Pei, C.L. Briant, H. Kesari, A.F. Bower, and E. Chason, Kinetics of Sn whisker nucleation using thermally induced stress. *Scr. Mater.* 93, 16–19 (2014).
- E. Chason, F. Pei, C.L. Briant, H. Kesari, and A.F. Bower, Significance of nucleation kinetics in Sn whisker formation. *J. Electron. Mater.* 43, 4435–4441 (2014).
- K.N. Tu and R.D. Thompson, Kinetics of interfacial reaction in bimetallic CuSn thin films. *Acta Metall.* 30, 947–952 (1982).
- C.H. Su, H. Chen, H.Y. Lee, and A.T. Wu, Controlled positions and kinetic analysis of spontaneous tin whisker growth. *Appl. Phys. Lett.* 99, 131906 (2011).
- L. Reinbold, N. Jadhav, E. Chason, and K.S. Kumar, Relation of Sn whisker formation to intermetallic growth: results from a novel Sn-Cu 'bimetal ledge specimen.' *J. Mater. Res.* 24, 3583–3589 (2009).
- F. Pei, A.F. Bower, and E. Chason, Quantifying the rates of Sn whisker growth and plastic strain relaxation using thermallyinduced stress. *J. Electron. Mater.* 45, 21–29 (2016).
- E. Chason and F. Pei, Measuring the stress dependence of nucleation and growth processes in Sn whisker formation. *JOM* 67, 2416–2424 (2015).
- P. Jagtap and P. Kumar, Manipulating crystallographic texture of Sn coatings by optimization of electrodeposition process conditions to suppress growth of whiskers. *J. Electron. Mater.* 44, 1206–1219 (2015).
- D. Susan, J. Michael, R.P. Grant, B. McKenzie, and W.G. Yelton, Morphology and growth kinetics of straight and kinked tin whiskers. Metall. *Mater. Trans. A Phys. Metall. Mater. Sci.* 44, 1485–1496 (2013).



- 62. N. Jain, X. Wang, P. Jagtap, A. Bower, and E. Chason, Analysis of pressure-induced whisker nucleation and growth in thin Sn films. *J. Electron. Mater.* 50, 6639–6653 (2021).
- 63. J.W. Shin and E. Chason, Stress behavior of electroplated Sn films during thermal cycling. *J. Mater. Res.* 24, 1522–1528 (2009).
- 64. V. Borra, O. Oudat, D.G. Georgiev, V.G. Karpov, and D. Shvydka, Metal whisker growth induced by localized, high-intensity DC electric fields. *MRS Adv.* 3, 3367–72 (2018).
- A.C. Vasko, G.R. Warrell, E.I. Parsai, V.G. Karpov, and D. Shvydka, Electron beam induced growth of tin whiskers. *J. Appl. Phys.* 118, 125301 (2015).
- P. Eckold, M.S. Sellers, R. Niewa, and W. Hügel, The surface energies of β-Sn — a new concept for corrosion and whisker mitigation. *Microelectron. Reliab.* 55, 2799–2807 (2015).
- 67. C.C. Wei, P.C. Liu, C. Chen, J.C.B. Lee, and I.P. Wang, Relieving Sn whisker growth driven by oxidation on Cu leadframe by

- annealing and reflowing treatments. J. Appl. Phys. 102, 043521 (2007).
- Y. Liu, C. Lu, P. Zhang, J. Yu, Y. Zhang, and Z.M. Sun, Mechanisms behind the spontaneous growth of Tin whiskers on the Ti2SnC ceramics. *Acta Mater.* 185, 433–440 (2020).

**Publisher's Note** Springer Nature remains neutral with regard to jurisdictional claims in published maps and institutional affiliations.

Springer Nature or its licensor (e.g. a society or other partner) holds exclusive rights to this article under a publishing agreement with the author(s) or other rightsholder(s); author self-archiving of the accepted manuscript version of this article is solely governed by the terms of such publishing agreement and applicable law.

